

4-1-2012

Modeling of a New Structure of Precision Air Conditioning System Using Secondary Condenser for Rh Regulation

Aries Subiantoro

Electrical Engineering Department, Faculty of Engineering University of Indonesia, Depok 16424, Indonesia, biantoro@ee.ui.ac.id

Nasruddin Nasruddin

Mechanical Engineering Department, Faculty of Engineering University of Indonesia, Depok 16424, Indonesia

Feri Yusivar


Electrical Engineering Department, Faculty of Engineering University of Indonesia, Depok 16424, Indonesia

Muhammad Idrus Al-Hamid

Mechanical Engineering Department, Faculty of Engineering University of Indonesia, Depok 16424, Indonesia

Bagio Budiardjo

Follow this and additional works at: <https://scholarhub.ui.ac.id/mjt>
Electrical Engineering Department, Faculty of Engineering University of Indonesia, Depok 16424,

 part of the [Chemical Engineering Commons](#), [Civil Engineering Commons](#), [Computer Engineering Commons](#), [Electrical and Electronics Commons](#), [Metallurgy Commons](#), [Ocean Engineering Commons](#), and the [Structural Engineering Commons](#)

Recommended Citation

Subiantoro, Aries; Nasruddin, Nasruddin; Yusivar, Feri; Al-Hamid, Muhammad Idrus; and Budiardjo, Bagio (2012) "Modeling of a New Structure of Precision Air Conditioning System Using Secondary Condenser for Rh Regulation," *Makara Journal of Technology*. Vol. 16: Iss. 1, Article 11.

DOI: 10.7454/mst.v16i1.1287

Available at: <https://scholarhub.ui.ac.id/mjt/vol16/iss1/11>

This Article is brought to you for free and open access by the Universitas Indonesia at UI Scholars Hub. It has been accepted for inclusion in Makara Journal of Technology by an authorized editor of UI Scholars Hub.

MODELING OF A NEW STRUCTURE OF PRECISION AIR CONDITIONING SYSTEM USING SECONDARY CONDENSER FOR RH REGULATION

Aries Subiantoro¹, Nasruddin², Feri Yusivar¹, Muhammad Idrus Al-Hamid², and
Bagio Budiardjo¹

1. Electrical Engineering Department, Faculty of Engineering University of Indonesia, Depok 16424, Indonesia
2. Mechanical Engineering Department, Faculty of Engineering University of Indonesia, Depok 16424, Indonesia

E-mail: biantoro@ee.ui.ac.id

Abstract

A dynamic mathematical model for a new structure of precision air conditioning (PAC) has been developed. The proposed PAC uses an additional secondary condenser for relative humidity regulation compared to a basic refrigeration system. The work mechanism for this system and a vapour-compression cycle process of the system are illustrated using psychrometric chart and pressure-enthalpy diagram. A non-linear system model is derived based on the conservation of mass and energy balance principles and then linearized at steady state operating point for developing a 8th-order state space model suited for multivariable controller design. The quality of linearized model is analyzed in terms of transient response, controllability, observability, and interaction between input-output variables. The developed model is verified through simulation showing its ability for imitating the nonlinear behavior and the interaction of input-output variables.

Abstrak

Pemodelan Sistem Tata Udara Presisi Berstruktur Baru Menggunakan Kondenser Sekunder untuk Pengaturan RH. Tulisan ini membahas penurunan model matematis dinamis untuk sistem tata udara presisi (PAC) dengan struktur baru. Berbeda dengan sistem refrigerasi umumnya, sistem PAC yang diusulkan menggunakan kondenser sekunder tambahan untuk pengaturan kelembaban relatif. Mekanisme kerja dan proses siklus kompresi uap sistem ini diilustrasikan menggunakan psychrometric chart dan diagram tekanan-entalpi. Model nonlinier sistem diturunkan berbasis konservasi massa dan prinsip kesetimbangan energi dan kemudian dilinierisasi pada titik kerja untuk mengembangkan model ruang keadaan orde-8 yang cocok untuk disain pengendali multivariabel. Kualitas model linier dianalisa dari aspek respons transien, kontrolabilitas, observabilitas, dan interaksi antar variabel masukan-keluaran. Model yang dikembangkan diverifikasi secara simulasi menunjukkan kemampuan model untuk meniru karakteristik nonlinier dan interaksi variabel masukan-keluaran.

Keywords: modeling, multivariable model, precision air conditioning, vapour-compression cycle

1. Introduction

The Datacenter room is filled with various high density computer equipments that serve high priority works and must meet specific environment requirements. In order to achieve a good performance, temperature and relative humidity (RH) of the equipments must be maintained in a comfort area recommended by ASHRAE. Several problems, such as conductive anodic failures, tape media errors, excessive wear, short circuit, electrostatic discharge, and corrosion, may arise if the temperature and RH exceed the recommended limit. In recent

decades, precision air conditioning (PAC) systems are widely used in small- to medium Datacenter buildings to control the temperature of equipments in cabinets. PAC removes heat generated by the equipments using vapour-compression process cycle. Another problem encountered is that a large Datacenter can easily consume as much electrical power as a small city [1].

During the last decades, modeling, control, and vapor compression diagnosis have been the focus of various interesting research to improve control performance. Air conditioning systems have been conventionally

controlled using single-input-single-output techniques. The temperature of PAC system is usually controlled by manipulating variable speed compressor. Many researchers suggested various control strategy based on number of operating parameter [2-3], energy balance of air and refrigerant [4], and qualitative model [5]. However, research has demonstrated that this approach has numerous difficulties, and results in limited control performance such as large variation of temperature, tendency to be non-convergence, slow response, and non-zero steady state error. In [6] the interaction between variables is considered as a disturbance in the multi-loop control design, but the control has shown unsatisfactory performance due to neglecting cross-coupling between controlled variables.

Due to cross-coupling nature on system dynamics, only multivariable control strategies are able to satisfy multi objective control, such as temperature and RH, simultaneously. The design of multivariable control strategy requires a mathematical model of system which can imitate transient behavior and the interaction between variables. Tian and friends [7] suggest a fuzzy multivariable control but still ignore the interaction impact. Other methods using multivariable model obtained from the first principle concept [8-9], dynamic model reduction order [10], and low order identification model [11], have demonstrated that multivariable control can achieve satisfactory transient response on temperature and also enhance energy efficiency.

Original vapor compression cycle system generally uses an electric heater to manipulate the RH variable. In this paper, a new structure of precision air conditioning system is presented. Instead of electric heater, an additional secondary condenser which generates waste heat for regulating the RH variable is used. The proposed system has two outputs to be controlled

namely temperature and relative humidity by manipulating the variable speed compressor and a fan of secondary condenser. This paper is aimed at developing an accurate multivariable model for the new structure of air conditioning system, since the multivariable control performance highly depends on quality of the model. First, the work principle and a vapour-compression cycle of the PAC system are described using psychrometric chart and pressure-enthalpy (*P-h*) diagram. A nonlinear dynamic model is derived based on the conservation of mass and energy balance principles. In order to develop a multivariable linear model suited for multivariable controller design, the nonlinear model is linearized at steady state operating point using Taylor series. Analysis of the multivariable linear model in terms of transient response and cross couplings is also performed. Finally, the multivariable linear model is validated through simulation to investigate its ability in imitating the nonlinear behavior and cross-couplings between controlled variables.

2. Methods

Description of the Proposed PAC System. The new structure of precision air conditioning system shown in Figure 1 consists of a compressor, an evaporator, two condensers, two fans, a capillary pipe, an electronic valve, and a check valve. The PAC system is mainly composed of two parts, refrigerant-side and an air-side. The secondary condenser is placed at PAC outlet to work as an air heating coil. The working fluid of the PAC plant is refrigerant R134a, with a total charge of 0.5 kg.

The work principle of the PAC system can be described as follows. The temperature of the Datacenter room is assumed higher than the room temperature and RH level around 60%. As shown in figure 1, the fresh air from

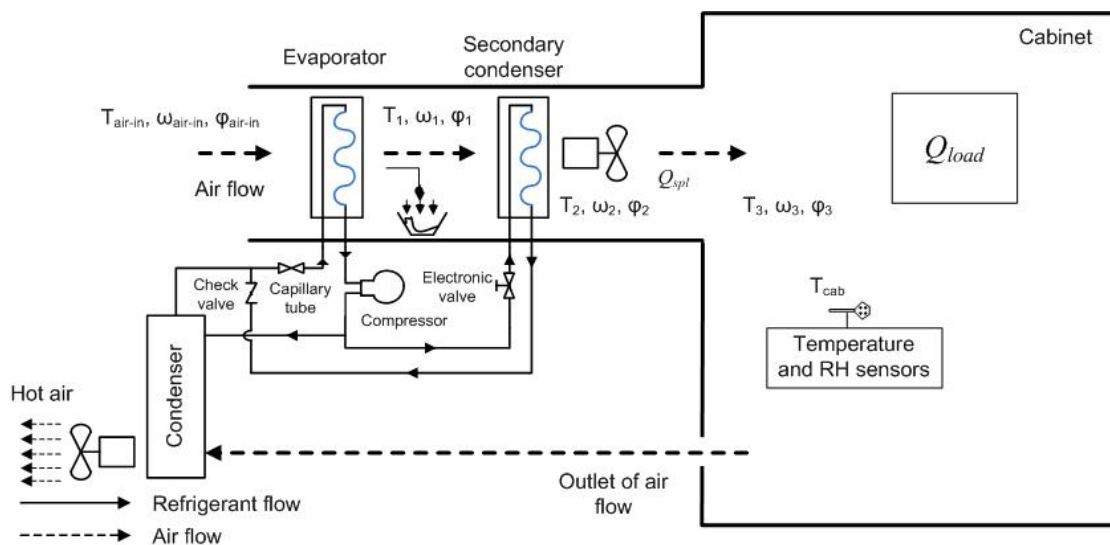


Figure 1. Schematic Representation of the Precision Air Conditioning System

Datacenter room is pulled inside the precision air conditioning system by the fix-speed fan. As the fresh air passes through the evaporator, heat transfer from air-side results in vaporation of the fresh air. The air leaving the evaporator is evaporated to a relatively low temperature T_1 and very high relative humidity ϕ_1 . The evaporator functions as a cooling coil. Next, the air passes through secondary condenser, where the refrigerant condenses and there is heat transfer from the refrigerant-side to the air-side. The waste heat from secondary condenser is used to raise the temperature and reduce the relative humidity, hence $T_2 > T_1$ and $\phi_1 > \phi_2$. In order to avoid the air temperature getting large, the refrigerant flow passing through the secondary condenser is limited only 10 percent from its maximum value. Considering heat generated by fix-speed fan Q_{sp} , the air temperature T_2 increases into T_3 at the outlet of PAC system. The air temperature T_3 and ϕ_3 must be maintained in the comfort zone to keep a good performance of computer equipments. The process of air conditioning is illustrated in a psychrometric chart shown in Figure 2.

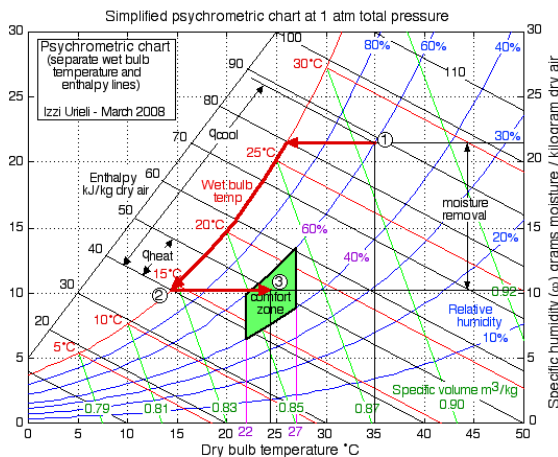


Figure 2. Psychrometric Chart of the PAC System

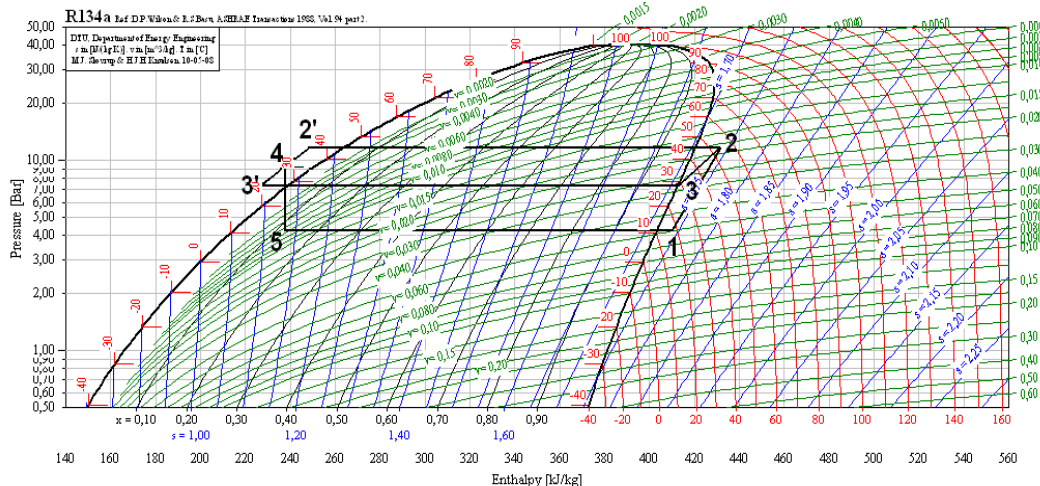


Figure 3. P-h Diagram Shows a Vapour-Compression Process Cycle for the PAC System

The Vapour-compression Process Cycle. The refrigerant flow passes through evaporator, compressor, condenser, secondary condenser, and capillary tube. The vapour-compression process cycle for the PAC system is described using the $P-h$ diagram shown in Figure 3 as follows: a) State point 1-2 is the compression process. At the inlet of compressor, the refrigerant is compressed increasing the temperature as well as the pressure, b) State point 2-2' is the condensation process in the first condenser. The refrigerant leaves the compressor with relative high temperature and flows into condenser coil by heat-transferring from its hot gaseous to the air-side. At constant pressure, refrigerant starts to condense and changes its phase from gas into liquid, c) State point 3-3' is the condensation process in the secondary condenser similar as occurred in the first condenser. The differences lie in the amount of refrigerant flow only 10% from maximum value and the condensation process performed at lower pressure. The temperature of refrigerant is higher than the air-side. The secondary condenser functions as a reheater where it enables a heat transfer from the hot refrigerant to the air-side. This causes the air temperature leaving the secondary condenser increases ($T_2 > T_1$) and the relative humidity decreases ($\phi_2 < \phi_1$). A variable-speed fan can help increasing the heat transfer by blowing air across the secondary condenser, d) State points 2'-4 and 3'-4 are the unification step of refrigerants leaving from the primary and secondary condensers. In order to overcome icing due to a pressure difference between the refrigerant flows of those condensers, a check valve is installed, e) Point 4-5 is the expansion process. The refrigerant flows through the capillary pipe which separates the high pressure side from the low pressure side. A large pressure drop is occurred causing some of the refrigerant to evaporate. Refrigerant changes from the liquid phase into two-phase region causing the temperature to drop down, f) State point 5-1 is the evaporation process. In the evaporator, a heat transfer

from the Datacenter room to the refrigerant is enabled by the low inlet refrigerant temperature. The heat from Datacenter room is absorbed and the remaining part of the liquid refrigerant evaporates at a constant temperature, and changes from liquid phase to gas phase. All refrigerant leaving the evaporator has evaporated and the air temperature has decreased slightly. The air temperature leaving the evaporator T_1 is lower than the air temperature of the Datacenter room T_{air-in} , but the relative humidity is going larger and saturated at $\phi_1 = 95\%$ -100%. The vapour-compression process cycle is now completed and the refrigerant returns to the inlet of the compressor, state point 1.

Modeling of Dynamic PAC System. Based on the work of Qi and Deng [11], the dynamic mathematical model for the PAC system can be derived from the energy and mass conservation principles by considering several assumptions, (1) the air side of the PAC evaporator includes dry-cooling region and wet-cooling region with volume ratio of 1:4, (2) the air side of the PAC condenser only includes the dry-cooling region, (3) the heat load of equipments inside the cabinet is considered constant, and (4) the heat losses in the air flow area is negligible.

As shown in Figure 1, the supply air from Datacenter room pulled by a fan flows through the evaporator and the secondary condenser until enters inside the cabinet. In this case, there is no need for a mathematical model of the primary condenser, since all informations required describing the behavior of the temperature and RH of the cabinet (T_{cab} , ϕ_{cab}) are available.

Compressor Model. It is assumed that the compressor is modeled as a static component. The refrigerant mass flow rate M_{ref} is calculated using equation 1 at constant condensing pressure and evaporating pressure

$$M_{ref} = \frac{s V_{com}}{v_s} \left(1 - 0,015 \left[\left(\frac{P_c}{P_e} \right)^{\frac{1}{\beta}} - 1 \right] \right) \quad (1)$$

The swept volume of the rotor compressor V_{com} is calculated using following equation $V_{com} = \frac{V_d}{n_c}$ (2)

where V_d and n_c are the displacement volume and the number of cylinder, respectively.

$$C_{pu} \rho_u V_1 \frac{dT_1'}{dt} = C_{pu} \rho_u f (T_{air-in} - T_1') + UA_1 \left(T_{we} - \frac{T_{air-in} + T_1'}{2} \right) \quad (3)$$

$$C_{pu} \rho_u V_2 \frac{dT_1}{dt} + \rho_u V_2 h_{fg} \frac{d\omega_1}{dt} = C_{pu} \rho_u f (T_1' - T_1) + C_{pu} f h_{fg} (\omega_{air-in} - \omega_1) + UA_2 \left(T_{we} - \frac{T_1' + T_1}{2} \right) \quad (4)$$

$$C_{pw} \rho_w V_{we} \frac{dT_{we}}{dt} = UA_1 \left(\frac{T_{air-in} + T_1'}{2} - T_{we} \right) + UA_2 \left(\frac{T_1' + T_1}{2} - T_{we} \right) - M_{ref} (h_{oe} - h_{ie}) \quad (5)$$

Evaporator Model. Figure 4 shows a schematic diagram of the evaporator where the air-side is divided into the dry region and the wet region. At the air-side of the evaporator, the temperature and the specific humidity entering the evaporator from Datacenter room are T_{air-in} and ω_{air-in} , respectively. Along the evaporator wall, the air temperature will decrease and equal to T_1' at the end of dry region, and the temperature of evaporator wall is assumed to be constant T_{we} . The differential equation for the dry region is determined using the energy balance principle shown in equation 3.

Meanwhile, in the wet-cooling region there is not only sensible heat transfer between the air and evaporator wall but also latent heat transfer. Applying the energy balance, the differential equation in the wet region can be described in terms of the air temperature and specific humidity as shown in equation 4.

The dynamic response on the refrigerant-side is much faster than on the air-side. If changes applied on both sides, the air-side is still in transient response phase while the refrigerant-side is already in the steady-state condition for a quite while. Therefore, the refrigerant mass flow rate along evaporator wall is assumed to be constant. The differential equation for the evaporator wall can be described based on the energy balance principle as shown in equation 5.

It is assumed that the air leaving the evaporator is saturated at 95%. Using linear regression method, the relationship between the temperature T_1 and the specific humidity ω_1 can be approximated by a 2nd order polynomial equation as follows

$$\omega_1 = 2.2427 \times 10^{-5} T_1^2 + 5.2878 \times 10^{-5} T_1 + 0.0041 \quad (6)$$

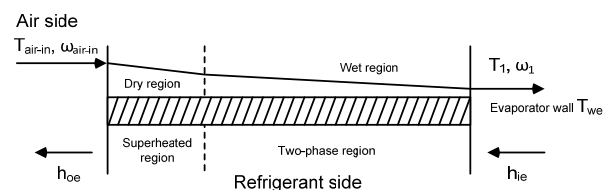


Figure 4. Schematic Diagram of the Evaporator

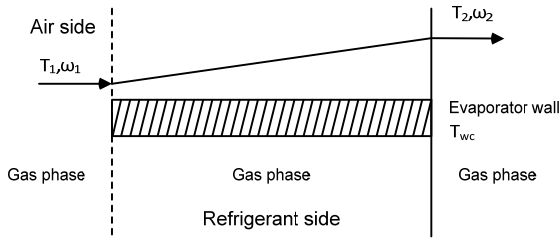


Figure 5. Schematic Diagram of Air Flow Inside the Secondary Condenser

Applying the first derivative on both sides of equation 6, a nonlinear differential equation for relating between the specific humidity and the temperature leaving the evaporator is expressed as follows

$$\frac{d\omega_1}{dt} = \frac{(4.4854T_1 + 5.2878) dT_1}{10^5 dt} \quad (7)$$

Secondary Condenser Model. Unlike the evaporator, the secondary condenser has only dry-cooling region as shown in figure 5. A heat transfer from the refrigerant to the air side is enabled by the hot refrigerant temperature at the inlet of the secondary condenser. Hence, the air temperature is increased along the secondary condenser and equal to the waste heat T_2 . The waste heat is then used to reduce the moisture content at the end of air-side. In order to prevent raising the air temperature, the refrigerant mass flow rate passing through the secondary condenser is determined only a small fraction of the total of refrigerant mass flow rate, $M_{ref2}=0,1M_{ref}$. The derivation of mathematical model for the secondary condenser is similar to the evaporator dry region. The energy balance for the air side and the secondary condenser wall can be written as differential equations in equation 8 and 9, respectively.

$$C_{pu}\rho_u V_{w2} \frac{dT_2}{dt} = C_{pw}\rho_w f(T_1 - T_2) + UA_3 \left(T_{wc} - \frac{T_1 + T_2}{2} \right) \quad (8)$$

$$C_{pw}\rho_w V_{w2} \frac{dT_{wc}}{dt} = UA_3 \left(\frac{T_1 + T_2}{2} - T_{wc} \right) - M_{ref2}(h_{o2} - h_{i2}) \quad (9)$$

Cabinet Model. The air at the end of PAC system is pulled in by a variable-speed fan entering the cabinet space to regulate the cabinet temperature T_{cab} . The variable-speed fan generates load heat causing the air temperature increases. Therefore, a mathematical model for the supply air at the inlet of cabinet space is given by following equation

$$T_3 = \frac{C_{pu}\rho_u f T_2 + \dot{Q}_{spl}}{C_{pu}\rho_u f} \quad (10)$$

It is assumed that no humidity load generated by the fan. Hence, the specific humidity leaving the fan ω_3 is considered equal to the specific humidity leaving the

secondary condenser ω_2 . Applying the energy balance principle, a mathematical model for the conditioned cabinet space can be described by the following differential equation

$$C_{pu}\rho_u V_{cab} \frac{dT_{cab}}{dt} = C_{pu}\rho_u f(T_3 - T_{cab}) + Q_{load} \quad (11)$$

Meanwhile, the moisture mass balance inside the cabinet is given by

$$\rho_u V_{cab} \frac{d\omega_{cab}}{dt} = \rho_u f(\omega_3 - \omega_{cab}) + M \quad (12)$$

where M is the moisture load generation in the cabinet.

The controlled variables are the temperature of cabinet T_{cab} and the relative humidity of cabinet ϕ_{cab} . The relationship between the relative humidity ϕ_{cab} and the specific humidity ω_{cab} is calculated using equations 13-14 as follows

$$\phi_{cab} = \frac{\omega_{cab} P}{(0.622 + \omega_{cab}) P_g} \quad (13)$$

$$P_g = 0.6108 \exp\left(\frac{17.27 T_{cab}}{T_{cab} + 237.3}\right) \quad (14)$$

3. Results and Discussion

In this section, the developed model of PAC system will be analyzed in terms of the characteristics of transient response and the cross-couplings between variables. First, the nonlinear model is linearized at a certain operating point in order to derive a linear multivariable model. Based on the linear model, the characteristics of the model such as the eigenvalues, controllability, and observability can be determined. The analysis results are useful especially for the controller- and observer- design

Table 1. Parameter Values of PAC

Parameter	Numerical Value	Parameter	Numerical Value
C_{pu}	1.005 kJ/kg	C_{pw}	0.385 kJ/kg
ρ_u	1.18 kg/m ³	ρ_w	8940 kg/m ³
V_1	0.000129 m ³	V_{we}	0.000645 m ³
V_2	0.000516 m ³	V_{wc2}	0.001305 m ³
V_{cab}	1 m ³	h_{fg}	2450 kJ/kg
UA_1	0.00508 kW/°C	UA_3	0.028416 kW/°C
UA_2	0.02032 kW/°C	F	0.04722 m ³ /s
T_{air-in}	25 °C	ω_{air-in}	0.01291 kg/kg
V_d	0.0000025 m ³	n_c	1
\square	1.2	v_s	0.05 m ³ /kg
P_c	1165.723 kPa	P_e	424.0417 kPa
h_{ie}	237.57 kJ/kg	h_{ic2}	412.37 kJ/kg
h_{oe}	409.922 kJ/kg	h_{oc2}	225.137 kJ/kg
Q_{spl}	0.01 kW	Q_{load}	0.3 kW
M	0.01/50 kg/s	P	101.325 kPa

purpose. An issue only encountered in the multivariable systems is the cross-coupling effect. This aspect will also be analyzed for the PAC system which is belonged to a multivariable system.

The parameters used to simulate the PAC model are shown in Table 1. These parameters are determined based on the equipment specification, the physical properties of material, and based on experiment tests combined with calculation using CoolPack program, with the following assumptions: a) C_{pu} , ρ_u and P are the general constant, the latent heat air vaporation h_{fg} , and the hermetic reciprocating β compressor type index referred to Qi and Deng [12]; b) C_{pw} and ρ_w are obtained from physical property of the evaporator's wall material and secondary condenser made from copper; c) V_1 , V_2 , V_{we} , V_{wc2} , V_d , n_c , and f are obtained from equipment's specification; d) UA_1 , UA_2 and UA_3 are obtained from manufacturers' data of evaporator and condensers; e) M is the humidity load of perfectly sealed cabinet and assumed as a small value; f) v_s , P_c , P_e , h_{ie} , h_{oe} , h_{ic2} and h_{oc2} are obtained from experiment combined with calculation using CoolPack program.

$$\dot{\mathbf{x}} = \mathbf{G}^{-1}\mathbf{f}_1(\mathbf{x}, \mathbf{u}, t) \tag{15}$$

Expressions of all elements in matrix \mathbf{G} and \mathbf{f}_1 are given in the appendix A. The linear model is derived about the operating point $(\mathbf{x}^0, \mathbf{u}^0)$ as described in table 2 using Taylor series method

$$\begin{aligned} \dot{\mathbf{x}} &= \mathbf{G}^{-1} \left[\frac{\partial \mathbf{f}_1}{\partial \mathbf{x}} \Big|_{\mathbf{x}^0, \mathbf{u}^0} \mathbf{x} + \frac{\partial \mathbf{f}_1}{\partial \mathbf{u}} \Big|_{\mathbf{x}^0, \mathbf{u}^0} \mathbf{u} + \frac{\partial \mathbf{f}_1}{\partial \mathbf{n}} \Big|_{\mathbf{x}^0, \mathbf{u}^0} \mathbf{n} \right] \\ &= \mathbf{A}(\mathbf{x}^0, \mathbf{u}^0) \mathbf{x} + \mathbf{B}(\mathbf{x}^0, \mathbf{u}^0) \mathbf{u} + \mathbf{V}(\mathbf{x}^0, \mathbf{u}^0) \mathbf{n} \end{aligned} \tag{16}$$

and the values of system model matrix obtained are

$$\mathbf{A}(\mathbf{x}^0, \mathbf{u}^0) = \begin{bmatrix} -0.0079 & 0 & 0 & 0 & 0.0079 & 0 & 0 & 0 \\ 0 & -0.0079 & 0 & 0 & 0 & 0 & 0 & 0.0079 \\ 0 & 0 & -19.3249 & -0.7375 & 0 & 20.0624 & 0 & -0.0057 \\ 0 & 0 & 0 & -78.1338 & 0 & 33.2067 & 0 & 0 \\ 0 & 0 & -3.0984 & 0 & -15.263 & 0 & 18.3613 & 0 \\ 0 & 0 & 0.0046 & 0.0057 & 0 & -0.0114 & 0 & 0 \\ 0 & 0 & 0.0032 & 0 & 0.0032 & 0 & -0.0063 & 0 \\ 0 & 0 & -0.0208 & -0.0008 & 0 & 0.0216 & 0 & -6.0889 \end{bmatrix}$$

Linearization of Nonlinear Model. A set of the first order of nonlinear differential equation (1)-(16) represents the dynamic model of PAC system. The model contains the knowledge of the characteristics of the system which are needed in the design of multivariable control. The nonlinear differential equations must be linearized about the operation point $(\mathbf{x}^0, \mathbf{u}^0)$ to obtain a linear state space model in order to simplify the controller design,

Define the vector of state variables as $\mathbf{x} = [T_{cab}, \omega_{cab}, T_1, T_1', T_2, T_{we}, T_{wc2}, \omega_1]^T$ and the inputs vector $\mathbf{u} = [s, f]^T$, the disturbance vector $\mathbf{n} = [T_{air-in}, \omega_{air-in}, Q_{load}]$, and the output vector as $\mathbf{y} = [T_{cab}, \phi_{cab}]$. Combining equations 1, 3-5, 7-9, 11-13, the developed equations of PAC system is expressed with the following compact state space form

$$\begin{aligned} \mathbf{B}(\mathbf{x}^0, \mathbf{u}^0) &= \begin{bmatrix} -1.7868 & 0 \\ -0.0002 & 0 \\ 3855.6 & 0 \\ 14719 & 0 \\ -760.3846 & 0 \\ 0 & -0.0038 \\ 0 & 0.00020549 \\ 4.1377 & 0 \end{bmatrix} \tag{17} \\ \mathbf{V}(\mathbf{x}^0, \mathbf{u}^0) &= \begin{bmatrix} 0.08432 & 0 & 0 & 0 \\ 0 & 0.8475 & 0 & 0 \\ 0 & 0 & 62410 & 0 \\ 0 & 0 & 0 & 349.3778 \\ 0 & 0 & 0 & 0 \\ 0 & 0 & 0 & 0.0012 \\ 0 & 0 & 0 & 0 \\ 0 & 0 & 66.0886 & 0 \end{bmatrix} \end{aligned}$$

The equation of system output is calculated using linear regression method based on a linear relationship between the relative humidity of cabinet and the specific humidity of cabinet as follows

$$\phi_{cab} = c_0 + c_1 T_{cab} + c_2 \omega_{cab} \tag{18}$$

For a set of data of the relative humidity and the specific humidity $\{\phi_{cab}(i), \omega_{cab}(i)\} \ i=1, \dots, N$, the equation 18 can be described in the form of regression equation

$$\underbrace{\begin{bmatrix} \phi_{cab}(1) \\ \phi_{cab}(2) \\ \vdots \\ \phi_{cab}(N) \end{bmatrix}}_{\mathbf{Y}} = \underbrace{\begin{bmatrix} 1 & T_{cab}(1) & \omega_{cab}(1) \\ 1 & T_{cab}(2) & \omega_{cab}(2) \\ \vdots & \vdots & \vdots \\ 1 & T_{cab}(N) & \omega_{cab}(N) \end{bmatrix}}_{\mathbf{\Phi}} \underbrace{\begin{bmatrix} c_0 \\ c_1 \\ c_2 \end{bmatrix}}_{\mathbf{\theta}} \tag{19}$$

Applying the least squares formula, the parameter vector $\mathbf{\theta}$ is determined using following equation

$$\hat{\mathbf{\theta}} = (\mathbf{\Phi}^T \mathbf{\Phi})^{-1} \mathbf{\Phi}^T \mathbf{Y} \tag{20}$$

and yields the parameters $c_0=0.7687$, $c_1=-0.0299$, dan $c_2=46.9$. Therefore, the output of the PAC system can be written as

$$\begin{aligned} \mathbf{y} &= \mathbf{f}_2(\mathbf{x}, \mathbf{u}, t) \\ &= \mathbf{C}(\mathbf{x}^0, \mathbf{u}^0) \mathbf{x} + \mathbf{d} \end{aligned} \tag{21}$$

where

$$\mathbf{C}(\mathbf{x}^0, \mathbf{u}^0) = \begin{bmatrix} 1 & 0 & 0 & 0 & 0 & 0 & 0 & 0 \\ -0.0299 & 46.9 & 0 & 0 & 0 & 0 & 0 & 0 \end{bmatrix}$$

$$\mathbf{d} = \begin{bmatrix} 0 \\ 0.7687 \end{bmatrix} \quad (22)$$

The characteristics of PAC system model are obtained by calculating the eigenvalues of system matrix \mathbf{A} resulting in $\lambda = [-0.0472, -0.0472, -382.72, -96.29, -45.54, -0.04, -0.01, -0.005]^T$. All the eigenvalues are located on the left side of the s -plane which implies that the open loop response of the linearized model is asymptotically stable. It is also shown that the PAC system has 5 dominant poles closed to the origin point $s=0$ showing a slow transient response from changes in the given set point or the unmeasured disturbance.

The main use of the model is to design the controller which guides the state variables to their final values at a suitable time. If a modern multivariable control strategy such as MPC or LQG is employed, a test for controllability is necessary in order to measure the number of the eigenvalues that can be moved away from the origin point. The controllability test describes that the state variable \mathbf{x} are able to be guided to the final value of states \mathbf{x}_e with the suitable control signal by evaluating the controllability matrix

$$\mathbf{Q}_c = [\mathbf{B} \quad \mathbf{AB} \quad \dots \quad \mathbf{A}^{n-1}\mathbf{B}] \quad (23)$$

Since $\text{rank}\{\mathbf{Q}_c\}=8$ has a maximum value, it means that the multivariable controller can move all eigenvalues λ to improve the control performance.

The application of multivariable state space controller needs information about the state variable \mathbf{x} in order to calculate the control signal \mathbf{u} . Since only sensors for the output of PAC system \mathbf{y} are available, the other 7 state variables must be estimated based on the measured input-output data using an observer. The unknown initial value of states \mathbf{x}_0 can be perfectly estimated by the observer, if the matrix \mathbf{Q}_o for testing the observability

$$\mathbf{Q}_o = \begin{bmatrix} \mathbf{C} \\ \mathbf{CA} \\ \vdots \\ \mathbf{CA}^{n-1} \end{bmatrix} \quad (24)$$

has a full rank number. For the model of PAC system, the rank of the controllability matrix \mathbf{Q}_o is maximum equal to the number of state variable $n=8$. All of unmeasured state variables will be known exactly even only sensors for measuring the output available.

Analysis of Cross-Couplings. The PAC system has two interacting control loops between s - T_{cab} and $f\phi_{cab}$. In order to measure the interaction among these control loops, an analytical tool called the relative gain array

(RGA) method can be used which is defined in terms of matrix operation as follows

$$\mathbf{\Lambda} = \mathbf{K} \cdot (\mathbf{K}^T)^{-1} \quad (25)$$

where the sign of (\cdot) is a product of Hadamard. The gain matrix \mathbf{K} consists of static gain value of each sub-system

$$\mathbf{K} = \begin{bmatrix} K_{11} & K_{12} & \dots & K_{1n} \\ K_{21} & K_{22} & \dots & K_{2n} \\ \vdots & & \ddots & \vdots \\ K_{n1} & K_{n2} & \dots & K_{nn} \end{bmatrix} \quad (26)$$

with K_{ij} defined as DC gain of transfer function G_{ij}

$$K_{ij} = \lim_{s \rightarrow 0} G_{ij}(s) \quad (27)$$

Each element in matrix $\mathbf{\Lambda}$, denoted λ_{ij} , describes the ratio between the open loop static gain from input u_j to output y_i and the gain between the same variables when all other loops are perfectly controlled

$$\lambda_{ij} = \frac{\left. \frac{\partial y_i}{\partial u_j} \right|_{u_{k \neq j}}}{\left. \frac{\partial y_i}{\partial u_j} \right|_{y_{k \neq i}}} \quad (28)$$

If λ_{ij} value is closer to 1 indicates a weak interaction between the i - j loops and all other loops. If λ_{ij} is a large positive number, it implies that the i - j loop gain will be attenuated substantially under diagonal control. If the value of λ_{ij} is negative, then it indicates a positive feedback and quite possibly unstable behavior.

To analyze the interaction variables for the PAC system with 2-inputs-2-outputs, the RGA for $\mathbf{K}_{2 \times 2}$ is found to be

$$\mathbf{\Lambda}_{2 \times 2} = \begin{bmatrix} 19.1473 & -18.1473 \\ -18.1473 & 19.1472 \end{bmatrix}$$

The value of λ_{ii} for control loop s - T_{cab} and $f\phi_{cab}$ are both 19.1473, indicating that the cross-coupling between both loops may affect an attenuation in both

Table 2. The Operating Point ($\mathbf{x}^0, \mathbf{u}^0$) of the PAC System

Variable	Numerical Value	Variable	Numerical Value
$T_{cab,0}$	25.2051 °C	$\omega_{cab,0}$	0.0104 kg/kg
$T_{1,0}$	22.4299 °C	$T_{1,0}$	23.0859 °C
$T_{2,0}$	23.4183 °C	$T_{we,0}$	3.0266 °C
$\omega_{1,0}$	0.0102 kg/kg	$T_{wc,0}$	24.8727 °C
s_0	60 rps	f_0	0.04722

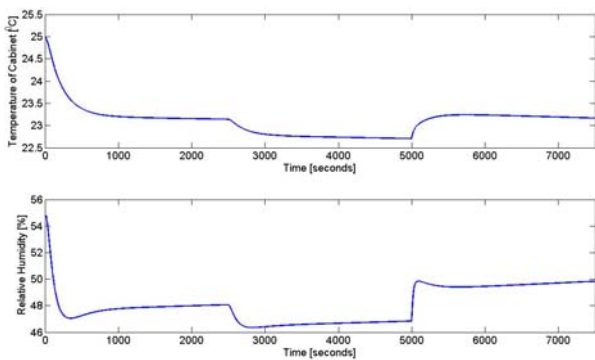


Figure 6. The Response of Cabinet Temperature (Above) and Cabinet Relative Humidity (Below)

loops. Due to the substantial interaction between the two SISO loops, the PAC system cannot be controlled by a multi-loop control which can guide the system into a non-zero steady-state error. It is clear from this cross-coupling analysis that only a multivariable control can significantly improve the control performance. Figure 12 shows the response of the cabinet temperature and the cabinet relative humidity to a step change in compressor speed and fan speed. As shown in the time interval 2500-5000 seconds, a change in the compressor speed while keeping the fan speed constant results in both temperature and relative humidity responses. Another interaction response is also shown when the fan speed changes and the compressor speed is constant in the time interval of 5000-7500 seconds as well.

Model Verification. In order to verify the linearized model sufficient in capturing the nonlinear behavior of the PAC system, the linear model is compared to the nonlinear model as shown in figure 7. The figures show open-loop response of the cabinet temperature and the cabinet relative humidity to step changes of compressor speed [50 rps, 60 rps] and fan speed [75%, 100%]. The output of linear model can simulate the output of nonlinear model good enough about the operating point $(\mathbf{x}^0, \mathbf{u}^0)$. The linear model produces an offset if the PAC system operates not closed to the determined operating point. In controller design, this offset normally will be eliminated using an integrator.

From the analysis results and the model verification, we can see that the multivariable model that was developed using a linearization process about the operating point $(\mathbf{x}^0, \mathbf{u}^0)$ is able to mimic the characteristics of the nonlinear model at steady state condition with sufficient accuracy. There is still an offset encountered between the the linear model response and the nonlinear model response due to simplification of the process complexity, but the tendency of both models are consistent. Hence, this multivariable state-space model of the PAC system, is a good representation for

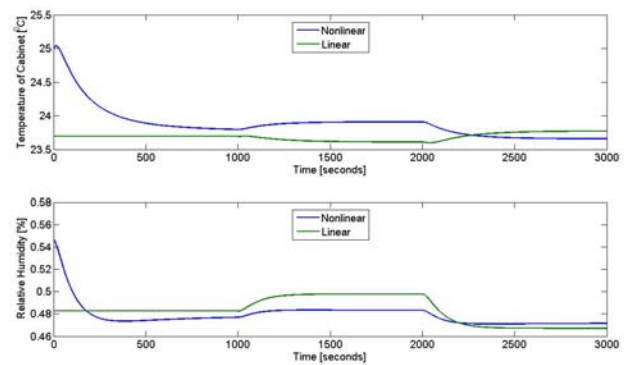


Figure 7. Validation between PAC Nonlinear Model and PAC Linier Model

describing the knowledge of the PAC system mathematically and also very suitable for multivariable controller design.

4. Conclusion

A nonlinear model for a new structure of precision air conditioning system using waste heat for RH regulation has been derived based on the conservation of mass and energy balance principle. The work of principle and the vapour-compression process cycle of this new PAC system are illustrated using psychrometric chart and the *P-h* diagram. A multivariable linear model is also derived about a certain operating point using Taylor series method and analyzed in terms of transient response and cross-coupling between control loops. The linear model is verified through simulation showing its capability to cope the nonlinear and cross-coupling behavior.

Acknowledgement

The authors would like to acknowledge the financial supports from University of Indonesia under Research Grant Scheme Riset Unggulan Universitas Indonesia Grant 2010 no. 2583/H2.R12/PPM.00.01 Sumber Pendanaan /2010.

Nomenclature

- M_{ref} : total refrigerant mass flow (kg/s)
- s : compressor speed (rps)
- V_{com} : swept volume compressor (m^3)
- v_s : specific volume of the superheat refrigerant (m^3/kg)
- P_c : condensation pressure (kPa)
- P_e : evaporation pressure (kPa)
- β : compression index
- V_d : displacement volume compressor (m^3)
- n_c : the number of cylinder in the compressor
- C_{pu} : specific air heat (kJ/kg °C)

C_{pw}	: specific heat in the evaporator wall (kJ/kg°C)	h_{ie}	: Enthalpy for evaporator input (kJ/kg)
ρ_u	: air density (kg/m ³)	h_{oe}	: Enthalpy for evaporator output (kJ/kg)
ρ_w	: evaporator wall/condenser density (kg/m ³)	UA_2	: overall heat transfer in the secondary condenser (kW/°C)
V_1	: volume of air side in the dry region (m ³)	T_2	: air temperature of secondary condenser (°C)
V_2	: volume of air side in the wet region (m ³)	T_{wc2}	: secondary condenser wall temperature (°C)
V_{we}	: evaporator air side total volume (m ³)	M_{ref2}	: refrigerant mass flow in the secondary condenser (kg/s) ($M_{ref2}=0.1 \times M_{ref}$)
f	: air flow speed (m ³ /s)	h_{ic2}	: enthalpy of secondary condenser input (kJ/kg)
h_{fg}	: latent heat from the air vaporation (kJ/kg)	h_{oc2}	: enthalpy of secondary condenser output (kJ/kg)
UA_1	: heat transfer from evaporator dry region (kW/°C)	V_{wc2}	: secondary condenser air side volume (m ³)
UA_2	: heat transfer from evaporator wet region (kW/°C)	T_2	: air temperature before passing the fan (°C)
ω_{air-in}	: specific air humidity in the Datacenter room (kg/kg)	Q_{spl}	: heat from the fan (kW)
ω_1	: specific humidity from evaporator output (kg/kg)	V_{cab}	: cabinet volume (m ³)
T_{air-in}	: air temperature in Datacenter room (°C)	Q_{load}	: heat sensible load from the IT equipment (kW)
T_1	: air temperature between the evaporator dry and wet region (°C)	M	: humidity load of the cabinet (kg/s)
T_1	: air temperature of evaporator output (°C)	P	: atmosphere pressure (kPa)
T_{we}	: evaporator wall temperature (°C)	P_g	: vapor saturation pressure (kPa)

Appendix-A

A set of nonlinear differential equations of the precision air conditioning can be written as follows

$$\underbrace{\begin{pmatrix} \dot{T}_{cab} \\ \dot{\omega}_{cab} \\ \dot{T}_1 \\ \dot{T}_1 \\ \dot{T}_2 \\ \dot{T}_{we} \\ \dot{T}_{wc2} \\ \dot{\omega}_1 \end{pmatrix}}_{\dot{\mathbf{x}}} = \underbrace{\begin{pmatrix} C_u \rho_u V_{cab} \\ \rho_u V_{cab} \\ b_2 + b_3 T_1 \\ C_{pu} \rho_u V_1 \\ C_{pu} \rho_u V_{wc2} \\ C_{pw} \rho_w V_{we} \\ C_{pw} \rho_w V_{wc2} \\ b_2 + b_3 T_1 \end{pmatrix}}_{\mathbf{G}^{-1}} \underbrace{\begin{pmatrix} C_{pu} \rho_u f (T_2 - T_{cab}) + \dot{Q}_{load} \\ \rho_u f (\omega_1 - \omega_{cab}) + M \\ C_{pu} \rho_u f (T_1' - T_1) + \rho_u f h_{fg} (\omega_{air-in} - \omega_1) + 0.5UA_2 (2T_{we} - T_1' - T_1) \\ C_{pu} \rho_u f (T_{air-in} - T_1') + 0.5UA_1 (2T_{we} - T_1' - T_{air-in}) \\ C_{pu} \rho_u f (T_1 - T_2) + 0.5UA_3 (2T_{wc2} - T_1 - T_2) \\ 0.5UA_1 (T_{air-in} + T_1' - 2T_{we}) + 0.5UA_2 (T_1' + T_1 - 2T_{we}) - a_1 s (h_{oe} - h_{ie}) \\ 0.5UA_3 (T_1 + T_2 - 2T_{wc2}) - 0.1a_1 s (h_{oc2} - h_{ic2}) \\ (a_2 T_1 + a_3) (C_{pu} \rho_u f (T_1' - T_1) + \rho_u f h_{fg} (\omega_{air-in} - \omega_1) + 0.5UA_2 (2T_{we} - T_1' - T_1)) \end{pmatrix}}_{\mathbf{f}_1(\mathbf{x}, \mathbf{u}, t)} \quad (\text{A-1})$$

where

$$\begin{aligned} b_2 &= C_{pu} \rho_u V_2 + \rho_u V_2 h_{fg} a_3 \\ b_3 &= \rho_u V_2 h_{fg} a_2 \end{aligned} \quad (\text{A-2})$$

The nonlinear model in equation (A-1) can be expressed in the following form

$$\dot{\mathbf{x}} = \mathbf{f}(\mathbf{x}, \mathbf{u}, t) \quad (\text{A-3})$$

Applying the Taylor series method to the nonlinear model in equation (A-1) about the operating point $(\mathbf{x}^0, \mathbf{u}^0)$ yields partial first derivation for state variables \mathbf{x} ,

$$\frac{\partial \mathbf{f}_1}{\partial \mathbf{x}} = \begin{bmatrix} (C_{pu}\rho_u V_{cab})^{-1}(C_{pu}\rho_u f_0(T_2 - T_{cab})) \\ (\rho_u V_{cab})^{-1}(\rho_u f_0(\omega_1 - \omega_{cab})) \\ b_6 T_1 + \frac{(C_{pu}\rho_u f_0 - 0.5UA_2)}{b_2 + b_3 T_{1,0}} T_1' + \frac{UA_2}{b_2 + b_3 T_{1,0}} T_{we} + \frac{-\rho_u f_0 h_{fg}}{b_2 + b_3 T_{1,0}} \omega_1 \\ (C_{pu}\rho_u V_1)^{-1}(- (C_{pu}\rho_u f_0 + 0.5UA_1) T_1' + UA_1 T_{we}) \\ (C_{pu}\rho_u V_{wc2})^{-1}((C_{pu}\rho_u f_0 - 0.5UA_3) T_1 - (C_{pu}\rho_u f_0 + 0.5UA_3) T_2 + UA_3 T_{wc2}) \\ (C_{pw}\rho_w V_{we})^{-1}((0.5UA_1 + 0.5UA_2) T_1' + 0.5UA_1 T_1 - (UA_1 + UA_2) T_{we}) \\ (C_{pw}\rho_w V_{wc2})^{-1}(0.5UA_3(T_1 + T_2 - T_{wc2})) \\ b_8 T_1 + \frac{b_9(C_{pu}\rho_u f_0 - 0.5UA_2)}{b_2 + b_3 T_{1,0}} T_1' + \frac{b_9 UA_2}{b_2 + b_3 T_{1,0}} T_{we} + \frac{-b_9 \rho_u f_0 h_{fg}}{b_2 + b_3 T_{1,0}} \omega_1 \end{bmatrix} \quad (A-4)$$

where

$$\begin{aligned} b_2 &= C_{pu}\rho_u V_2 + \rho_u V_2 h_{fg} a_3 \\ b_3 &= \rho_u V_2 h_{fg} a_2 \\ b_6 &= \frac{-C_{pu}\rho_u f_0 - 0.5UA_2}{b_2 + b_3 T_{1,0}} - b_3 \left(\frac{C_{pu}\rho_u f_0 (T_{1,0}' - T_{1,0}) - \rho_u f_0 h_{fg} \omega_{1,0} + 0.5UA_2 (2T_{we,0} - T_{1,0}' - T_{1,0})}{(b_2 + b_3 T_{1,0})^2} \right) \\ b_7 &= \frac{b_3 b_9 (C_{pu}\rho_u f_0 (T_{1,0}' - T_{1,0}) - \rho_u f_0 h_{fg} \omega_{1,0} + 0.5UA_2 (2T_{we,0} - T_{1,0}' - T_{1,0}))}{(b_2 + b_3 T_{1,0})^2} \\ b_8 &= \frac{a_2 (C_{pu}\rho_u f_0 (T_{1,0}' - T_{1,0}) - \rho_u f_0 h_{fg} \omega_{1,0} + 0.5UA_2 (2T_{we,0} - T_{1,0}' - T_{1,0})) - b_9 (C_{pu}\rho_u f_0 + 0.5UA_2)}{b_2 + b_3 T_{1,0}} - b_7 \\ b_9 &= \frac{a_2 T_{1,0} + a_3}{a_2 T_{1,0} + a_3} \end{aligned} \quad (A-5)$$

the control signal \mathbf{u} ,

$$\frac{\partial \mathbf{f}_1}{\partial \mathbf{u}} = \begin{bmatrix} (C_{pu}\rho_u V_{cab})^{-1}(C_{pu}\rho_u (T_{2,0} - T_{cab,0})f) \\ (\rho_u V_{cab})^{-1}(\rho_u (\varpi_{1,0} - \varpi_{cab,0})f) \\ \frac{C_{pu}\rho_u (T_{1,0}' - T_{1,0}) + \rho_u h_{fg} (\omega_{air-in} - \omega_{1,0})}{b_2 + b_3 T_{1,0}} f \\ (C_{pu}\rho_u V_1)^{-1}(C_{pu}\rho_u (T_{air-in} - T_{1,0}')f) \\ (C_{pu}\rho_u V_{wc2})^{-1}(C_{pu}\rho_u (T_{1,0} - T_{2,0})f) \\ (C_{pw}\rho_w V_{we})^{-1}(-a_1(h_{oe} - h_{ie})s) \\ (C_{pw}\rho_w V_{wc2})^{-1}(-0.1a_1(h_{oc} - h_{ic})s) \\ \frac{(a_2 T_{1,0} + a_3) C_{pu}\rho_u (T_{air-in} - T_{1,0}') + \rho_u h_{fg} (\omega_{air-in} - \omega_{1,0})}{b_2 + b_3 T_{1,0}} f \end{bmatrix} \quad (A-6)$$

and the disturbance \mathbf{n}

$$\frac{\partial \mathbf{f}_1}{\partial \mathbf{n}} = \begin{bmatrix} (C_{pu}\rho_u V_{cab})^{-1} \dot{Q}_{load} \\ (\rho_u V_{cab})^{-1} M \\ \frac{\rho_u f_0 h_{fg}}{b_2 + b_3 T_{1,0}} \omega_{air-in} \\ (C_{pu}\rho_u V_1)^{-1}((C_{pu}\rho_u f_0 - 0.5UA_1) T_{air-in}) \\ 0 \\ (C_{pw}\rho_w V_{we})^{-1}(0.5UA_1 T_{air-in}) \\ 0 \\ \frac{(a_2 T_{1,0} + a_3) \rho_u f_0 h_{fg}}{b_2 + b_3 T_{1,0}} \omega_{air-in} \end{bmatrix} \quad (A-7)$$

Reference

- [1] V. Sorell, ASHRAE Journal 49 (2007) 32.
- [2] M.J. Poort, C.W. Bullard, Int. J. Refrig. 29 (2006) 683.
- [3] L.O.S. Buzelin, S.C. Amico, J.V.C. Vargas, J.A.R. Parise, Int. J. Refrig. 28 (2005) 165.
- [4] Z. Li, S. Deng, Int. J. Refrig. 30 (2007) 113.
- [5] C. Aprea, R. Mastrullo, C. Renno, Int. J. Refrig. 27 (2004) 639.
- [6] L. Hua, S.K. Jeong, S.S. You, Int. J. Refrig. 29 (2009) 1067.
- [7] J. Tian, Q. Feng, R. Zhu, Int. J. Refrig. 49 (2008) 933.
- [8] X.D. He, S. Liu, H.H. Asada, J. Dyn. Syst. Meas. Control-Trans. ASME 119 (1997) 183.
- [9] D. Leducq, J. Guilpart, G. Trystram, Int. J. Refrig. 29 (2006) 761.
- [10] B.P. Rasmussen, A.G. Alleyne, J. Dyn. Syst. Meas. Control-Trans. ASME 126 (2004) 54.
- [11] J.L. Lin, T.J. Yeh, Int. J. Refrig. 30 (2007) 209.
- [12] Q. Qi, S. Deng, Int. J. Refrig. 31 (2008) 841.